Published in final edited form as:
Biogeochemistry. 2018 ; 138(2): 137–154. doi:10.1007/s10533-018-0436-z.

Differential effects of chronic and acute simulated seawater intrusion on tidal freshwater marsh carbon cycling

Ellen R. Herbert[1], **Joseph Schubauer-Berigan**[2], **Christopher B. Craft**[1]

[1]School of Public and Environmental Affairs, Indiana University, Bloomington, USA

[2]US Environmental Protection Agency, Office of Research and Development, National Risk Management Research Laboratory, Cincinnati, USA

Abstract

Tidal freshwater ecosystems experience acute seawater intrusion associated with periodic droughts, but are expected to become chronically salinized as sea level rises. Here we report the results from an experimental manipulation in a tidal freshwater *Zizaniopsis miliacea* marsh on the Altamaha River, GA where diluted seawater was added to replicate marsh plots on either a press (constant) or pulse (2 months per year) basis. We measured changes in porewater chemistry (SO_4^{2-}, Cl^-, organic C, inorganic nitrogen and phosphorus), ecosystem CO_2 and CH_4 exchange, and microbial extracellular enzyme activity. We found that press (chronic) seawater additions increased porewater chloride and sulfate almost immediately, and ammonium and phosphate after 2–4 months. Chronic increases in salinity also decreased net ecosystem exchange, resulting in reduced CO_2 and CH_4 emissions from press plots. Our pulse treatment, designed to mimic natural salinity incursion in the Altamaha River (September and October), temporarily increased porewater ammonium concentrations but had few lasting effects on porewater chemistry or ecosystem carbon balance. Our findings suggest that long-term, chronic saltwater intrusion will lead to reduced C fixation and the potential for increased nutrient (N, P) export while acute pulses of saltwater will have temporary effects.

Keywords

Carbon cycling; Saltwater intrusion; Methane; Carbon dioxide; Greenhouse gases; Extracellular enzyme activity

Introduction

Tidal freshwater marshes (TFMs) are influenced by astronomical tides but are defined as having salinities less than 0.5 psu (Barendregt et al. 2009). They are highly productive systems that support a diverse community of plant and animal species and higher carbon sequestration than their saline counterparts (Odum 1988; Hopkinson 1992; Barendregt et al. 2009; Craft 2007; Neubauer 2008). Climate change is predicted to alter patterns of precipitation and temperature regimes, changing the magnitude and frequency of droughts and tropical storms that lead to acute (pulse) seawater intrusion into freshwater habitat (Nijssen et al. 2001). Meanwhile, mean sea level is expected to increase between 0.38 and 2 m in the next 100 years (Parris et al. 2012; Church et al. 2013; Horton et al. 2014), pushing

seawater into historically freshwater areas such as tidal freshwater marshes. This chronic (press) seawater intrusion will likely be exacerbated by anthropogenic activities (damming, freshwater withdrawals) that reduce freshwater discharge (Prat and Ibanez 1995; Montagna et al. 2002).

Seawater intrusion can alter both C fixation and mineralization (Neubauer and Craft 2009; Herbert et al. 2015). Increased ionic concentrations lead to osmotic stress while microbial reduction of seawater SO_4^{2-} produces H_2S, both of which can be toxic to freshwater species (Nielsen et al. 2003; Lamers et al. 2013). Seawater intrusion has been observed to alter plant physiology (Madrid et al. 2012; Sutter et al. 2013; Johns et al. 2014), reduce plant productivity (Spalding and Hester 2007; Sutter et al. 2013; Hackney and Avery 2015) and alter plant species composition (Flynn et al. 1995; Neubauer et al. 2013). Freshwater vegetation may recover from short pulses of salinity but prolonged periods of increased salinity result in a shift to communities dominated by brackish species (Flynn et al. 1995; Spalding and Hester 2007; Sharpe and Baldwin 2012; Sutter et al. 2013).

Seawater also alters soil microbial community composition (Jackson and Vallaire 2009; Edmonds et al. 2009; Nelson et al. 2015) and soil biogeochemistry. The most well studied consequence of saltwater intrusion is reduced methane (CH_4) production and enhanced SO_4^{2-} reduction (Bartlett et al. 1987; Weston et al. 2006; Chambers et al. 2011; Poffenbarger et al. 2011; Segarra et al. 2013). Sulfate reduction yields more energy than CH_4 production (Lovley and Klug 1986) and increased SO_4^{2-} reduction following seawater intrusion is predicted to increase mineralization of soil organic matter. However, the literature contains mixed reports with some studies finding that seawater enhances mineralization (Weston et al. 2006, 2011; Chambers et al. 2013a), while others document no change (Marton et al. 2012). Chambers et al. (2011) observed greater C loss from pulsed compared to press salinity treatments. There are also a growing number of studies that show that seawater as a press (Weston et al. 2011) or pulse (Chambers et al. 2013b) can enhance CH_4 production in addition to CO_2 production. While SO_4^{2-} reduction has been the emphasis of many recent studies of seawater intrusion, increased availability of SO_4^{2-} is not the only factor in salinity-driven changes in C mineralization. Wetland type (freshwater vs. brackish), soil type (peat vs. mineral), and vegetation type can also affect wetland response to increased salinity.

The enzymatic hydrolysis of large organic compounds has been proposed as the putative rate-limiting step in microbial organic matter mineralization (Sinsabaugh and Moorhead 1994; Schimel and Weintraub 2003; Allison and Vitousek 2005) and has been linked to rates of C mineralization and CH_4 production in wetland soils (Sinsabaugh and Findlay 1995; Freeman et al. 1998; Neubauer et al. 2013; Morrissey et al. 2013). Correlations between extracellular enzyme activity and salinity along estuarine salinity gradients (Morrissey et al. 2014) as well as experimental salinity manipulations (Jackson and Vallaire 2009; Neubauer et al. 2013; Chambers et al. 2013a) indicate that enzyme activity plays a role in the response of C mineralization to seawater intrusion. Changes in salinity and SO_4^{2-} have also been observed to alter the availability of inorganic nutrients such as nitrogen (N) and phosphorus (P), which can also affect microbial abundance and activity (Giblin et al. 2010; Jun et al. 2013; Noe et al. 2013; Lamers et al. 2014).

Many assessments of the effect of seawater intrusion on TFMs C cycling rely on short-term laboratory incubations of bare soils. However, plants interact strongly with changes in subsurface biogeochemistry, including enzyme activity, C mineralization, nutrient availability and methanogenesis (Van Der Nat and Middelburg 1998; Kang and Freeman 1999; Neubauer et al. 2005; Sutton-Grier and Megonigal 2011). In one of the few studies that linked plant and microbial responses to salinity at the ecosystem scale Neubauer et al. (2013) showed that soil CO_2 production (excluding root respiration) increased in response to a short-term (3 days) salinity pulse but declined over time in response to long-term (3.5 years) salinity exposure. They attributed the long-term reduction in C mineralization to changes in plant productivity and species composition that decreased the quantity and quality of C available to mineralization pathways and to N-limitation of enzyme production.

We investigated the impacts of chronic (press) and acute (pulse) saltwater intrusion on a TFM dominated by giant cutgrass (*Zizaniopsis miliacea* (Michx.) Döll and Asch.), on the Altamaha River (GA). We amended plots with either press or pulse doses of low concentrations of seawater to elevate porewater salinities and measured changes in soil biogeochemistry and plant communities against freshwater-treated and control (no water addition) plots. Here we present data on changes in porewater chemistry, extracellular enzyme activity, and C gas flux due to pulse and press seawater addition from the first 2.5 years of the Seawater Addition Long Term Experiment (hereafter SALTEx). We hypothesize that press additions of seawater will increase porewater salinity, Cl^-, SO_4^{2-}, N, and P, enhance enzyme activity and organic matter mineralization, and reduce ecosystem productivity and CH_4 emissions. We expect to see similar changes in pulse plots during seawater additions, but hypothesize that upon a return to freshwater conditions porewater chemistry and biogeochemical process rates will return to baseline conditions without inducing major ecosystem changes.

Methods

Study site

The experimental site is located in an emergent TFM in Macintosh County, Georgia dominated by *Zizaniopsis miliacea, Ludwigia repens* J.R. Forst., *Pontederia cordata* L., and several *Polygonum* species. SALTEx consists of thirty 2.5 × 2.5 m plots arrayed over a 0.1 ha area of marsh (Fig. 1). Plots are separated by a 3 m buffer to minimize leakage between treatments and accessed via a network of raised boardwalks. Plots were assigned to 6 groups (blocks) based on average elevation. Within each block, plots were randomly assigned to one of 5 treatment groups: control, control with sides, fresh water (hereafter fresh), press salinity (hereafter press) or pulse salinity (hereafter pulse; n = 6 per treatment). “Control” plots are left unmanipulated as methodological controls. The remaining 24 plots were demarcated by pushing a 0.3 m (h) by 2.5 m (l) × 2.5 m (w) ridged corrugated polycarbonate frame 15 cm into the soil so that approximately 15 cm remain aboveground (Polygal multiwall sheeting, Plazit-Polygal Group, Gazit, Israel). Each frame contains two open holes at the soil surface to allow for the exchange of water, organisms and materials. The holes were plugged during dosing then removed the rest of the time to allow for tidal exchange. The frames were installed in March 2013 and the marsh was allowed to equilibrate for 13 months before

experimental water additions began. The “Control Sides” plots were included to assess the effects of the hydrologic barrier created by the frame and received no experimental water additions.

Experimental water additions were made 4 times per week starting in April 2014 by plugging the holes and flooding the plots with approximately 265 L of treatment water which was allowed to infiltrate into the soils before the plugs were removed. “Press” plots receive a brackish mixture of seawater and fresh river water at a salinity of 15 psu and “fresh” plots receive fresh Altamaha River water throughout the year. “Pulse” plots receive river water for 10 months a year (November–September) and brackish treatment water for 2 months (September and October), mimicking the timing of periodic natural saltwater intrusion into the freshwater reaches of the Altamaha during low flow conditions in the fall (Supplementary Fig. 6).

Starting in March 2015, we discontinued measurements from five plots (two control with sides, one fresh, and two press) because porewater salinities were not in the correct range due to consistent leakage from the plots (i.e., press plots were not maintaining ~ 5 psu salinity and the fresh and control with sides plots had salinities > 0.5 psu). These plots were not included in statistical analyses from July 2015 onward.

In 2015, a representative year in terms of river flow, the plots were inundated (i.e. flooded to the soil surface or more) 95% of the time based on water levels measured every 15 min at a well in the center of the experiment. The average depth of flooding at high tide was 25 cm which is considerably above the 15.5 cm height of the plot siding. During 2015, 69% of the high tides exceeded the height of the siding, indicating that the plots are still hydrologically connected with the surface water at the site. The amount of water added to each 2.5 by 2.5 m plot by the treatment additions was approximately 53,000 L/year which was 5% of the water added by the tides (1,056,000 L/year) that year, assuming tidal additions are equal to the summed volume of water arriving at each high tide, calculated as plot area mutiplied by maximum tide height for each semidiurnal tide of 2015.

The source waters (river water and sea water) mixed for dosing the press and pulse treatments were sampled periodically throughout the experiment to characterize their chemical composition (Table 1). As expected, seawater contained much higher salinity (22 psu) and sulfate (1914 mg/L) than river water (0.09 psu, 36 mg/L) whereas river water was higher in ammonium-N, nitrate-N, total N, total P, and dissolved organic carbon. The brackish treatment water’s chemical composition was intermediate to those of sea water and river water. A more detailed description of the site and the experimental design are available in Supplementary Material.

Porewater chemistry

Each plot is outfitted with 4 porewater sampling wells consisting of a porous sintered plastic cup extending from 10 to 35 cm below the soil surface (nominal pore size 40 μm; Porex Co. Fairburn, GA) attached to a PVC pipe outfitted with an airtight cap and Tygon tubing. Salinity is measured from at least one well in each plot once per week and all wells are measured once per month.

Porewater chemistry was sampled seasonally in spring (March or April), summer (July), fall (October) and winter (December or January) starting in December 2013 preceding the start of treatments. All samples were collected at least 24 h (two tidal cycles) after the most recent treatment water application. At each sampling, two randomly selected wells in each plot were sampled as described in Supplementary Information. Porewater subsamples for NH_4^+, NO_3^-/NO_2^- and PO_4^- analysis were shipped frozen on dry ice to the US EPA Office of Research and Development (Cincinnati, OH) and analyzed within 28 days of collection. Samples were analyzed using a Lachat QuikChem 8500 Flow Injection Analysis system (Hach Company, Loveland, CO, USA) using the indophenol blue complex for NH_4^+ (EPA ESF-SOP-0270), cadmium reduction/EDTA red complex for NO_3^-/NO_2^- (EPA ESF-SOP-029) and molybdate blue complex for reactive P (EPA ESF-SOP-026). We summed NH_4^+ and NO_3^- as total inorganic N (TIN). Subsamples for Cl^-, SO_4^{2-} and DOC were shipped frozen to Indiana University (Bloomington, IN). Porewater Cl^- and SO_4^{2-} were measured on a Dionex ICS-2000 Ion Chromatograph (Sunnyvale, CA) with an AS11-HC analytical column. DOC was analyzed via high-temperature oxidation using a Shimadzu TOC-V_{CPN} analyzer (Columbia, MD, USA). For all analyses, known standards and ultrapure deionized water blanks were run every 10 samples to ensure accuracy and to correct for instrumental drift.

Extracellular enzyme activity

One 5.08 cm diameter by 25 cm deep soil core was taken in one sub-plot (see Fig. 1) in June 2013 and then seasonally in concert with gas flux and porewater measurements from January 2014 to March 2015. Soils were homogenized in the field and then stored at − 80 °C. We assessed extracellular enzyme activities (EEA) for four C-acquiring enzymes, β-D-glucosidase (BG), 1,4-β-cellobiosidase (CBH), β-xyloxidase (XLY) and β−1,4-*N*-acetylglucosaminidase (NAG), using a fluorometric assay following protocols modified from Bell et al. (2013). Soil slurries were prepared from the − 80 °C preserved samples using 10 g of soil and 91 mL of 50 mM acetate buffer adjusted to the pH (5.8) of the field-moist soils. 800 μL of slurry was pipetted in triplicate into deep 96-well plates and incubated at room temperature for 3 h with 250 μL of 300 μM 4-methylmubelliferyl-linked (MUB) model substrate, 4-MUB β-D-glucopyranoside for BG, 4-MUB β-D-cellobioside for CBH, 4-MUB-β-D-xylopyranoside for XLY and 4-MUB N-acetyl-β-D-glucosaminide for NAG (Sigma-Aldrich Co. Ltd.). This substrate concentration was determined to be non-limiting over the course of a 3–4 h incubation in previous assays (unpublished data). Standard quench curves (0–100 μM) for individual soil were prepared in separate plates for MUB to account for difference in fluorescent quenching between soils. Following the incubation period, 250 μL samples of the supernatant were pipetted into a clear-bottom 96-well plate and fluorescence was quantified at 360 nm excitation and 460 nm emission wavelengths on a Synergy 2 plate reader (Bioteck, Winooski, VT, USA). Enzyme activity was calculated by regressing fluorescent intensity against standard quench curves for each soil and then calculating the change in MUB concentration over incubation time per gram dry soil.

Gas exchange measurements

Gas flux measurements were made in June, July, and October 2013 and then seasonally in concert with the enzyme and porewater measurements starting in January 2014. Flux

measurements were made from a 0.69 × 0.69 m square base placed inside one subplot, 15 cm from the plot frame (Fig. 1). A 0.9 m tall rigid translucent Polygal chamber was placed over the flux collar. An extension could be added to increase the chamber height to 1.8 m to allow for taller vegetation. Connections between chamber sections and the chamber lid were made gas-tight using a water-filled channel. Three small fans were mounted inside the chamber to ensure the chamber air was well mixed. Gas was pumped from one side of the chamber through black Viton tubing to a PP Systems EMG4 portable infrared gas analyzer with onboard data logger (IRGA; PP Systems, Amesbury, MA) to non-destructively measure CO_2 concentrations in the chamber and then the gas returned to the main gas flow. The IRGA was calibrated daily per the manufacturer's instructions with a 500 ppm CO_2 Scott™ standard (Air Liquide, Troy, MI) and the calibration was checked with three Scott™ standards (10, 100, 1000 ppm CO_2).

We simultaneously measured air temperature and photosynthetically active radiation (PAR) inside and outside the chamber. Soil temperature was measured adjacent to the chamber (PP Systems soil temperature probe). The chamber temperature was maintained within 1.5 °C of outside air temperature by pumping ice water through a copper heat-exchange coil. Flux measurements were generally made over the course of 1 week between peak PAR hours of 10 am–3 pm at low tide. The chamber was placed within the designated sub-plot (Fig. 1) and allowed to equilibrate for 25–30 min before the chamber top was sealed. Gas exchange was measured at full sun and 3 levels of shade (40, 70%, full dark) by covering the chamber with shade cloth (SunBlocker™) or a black polyethylene sheet. Temperature, PAR and CO_2 measurements were recorded every 30 s. For CH_4, every 4 min a 20 mL sample of gas was withdrawn from a Luer Lock fitting and injected into an N_2 flushed and evacuated 12 mL Exetainer vial (Labco Limited, Lampeter, UK) and stored under deionized water. Five to seven gas samples were taken over the course of the flux measurements.

Gas samples were analyzed for CO_2 and CH_4 within 1 month of collection using a Varian 450-GC (Varian/Agilent Technologies, Palo Alto/Santa Clara, CA, USA) equipped with a thermal conductivity detector for CO_2 and flame ionization detector for CH_4. The GC was calibrated daily with 4–5 certified Scott™ standards for each gas (AirLiquid, Troy, MI). Certified standard mixtures and blanks were run every 15 samples to ensure accuracy and correct for instrument drift. Analysis of stored standards showed there was no effect of the holding time on gas concentrations. The gas concentrations were corrected for dilution from sampling and expressed on an areal basis and then regressed against sampling time. Production rates were calculated using the slopes of the regression for the linear portion of the curve (≥ 5 points, general time 4–28 min). We did not include gas concentration below the minimum detection limit of the instrument in the regressions nor did we utilize regressions with $r^2 < 0.85$.

Gas flux modeling

We modified the C gas flux model of Neubauer et al. (2000) to calculate daily gas fluxes from measured rates. For each plot at each sampling, we calculated photosynthesis by summing gross ecosystem productivity (GEP; the uptake rate of CO_2 during the light incubation in mg C m^{-2} min^{-1}) and ecosystem respiration (ER; emission rate of CO_2 under

dark conditions in mg C m^{-2} min^{-1}). We then developed photosynthesis versus PAR curves for each plot on each sampling date by fitting a hyperbolic curve following Whiting et al. (1992). Because we had only one ER and one CH_4 rate for each sampling date, we developed temperature versus ER or CH_4 curves for each plot using measurements from the first 2 years of data collection (10 sampling dates $plot^{-1}$) following Neubauer (2013). We then modeled hourly flux rates using 15 min PAR and temperature data from a weather station at Sapelo Island, Georgia (http://gce-lter.marsci.uga.edu/portal/marshlanding.htm), ~ 16 km from the SALTEx site. Because we found that CH_4 emissions decreased ~ 30% under dark conditions, we multiplied hourly CH_4 rates by 0.7 for time periods when PAR was < 100 μE m^{-2} s^{-1}. Hourly flux data was summed to calculate daily (24 h) rates of GEP, ER, and CH_4. Net ecosystem productivity NEP (g C m^{-2} d^{-1}) was calculated as the difference between daily GEP and ER. Based on Neubauer et al. (2000) and Neubauer (2013), we did not alter flux rates due to tides. For the first year of treatments (April 2014–March 2015), we calculated annual fluxes by multiplying weighted fluxes over annual cycles using temperature and PAR data. For instance, July and August had similar observed temperature, standing biomass and PAR regimes and thus the July PAR-photosynthesis and temperature-ER relationships were applied for August. Following previous studies, we did not propagate the errors associated with the photosynthesis-PAR ($r^2 > 0.95$) or respiration-temperature curves ($r^2 > 0.85$) forward into the uncertainty estimates for our annual flux values and thus our annual flux calculations may underestimate standard error estimates.

Statistical analysis

All statistical analyses were performed in SAS 9.4 (2012, SAS institute, Cary, NC). Prior to statistical tests, we verified assumptions of normality and homoscedasticity. To meet these assumptions, data were log-transformed. For presentation, means and standard errors (SE) were back-transformed. Data from the 6 replicates of each treatment were analyzed using ANOVA for a randomized block design based on treatment, elevation, and sampling date, which tests for the effect of differences among the five treatments adjusting for the variation between elevation blocks. Treatment means were separated post-ANOVA using the Ryan-Einot-Welsch Multiple Range Test. All tests were conducted at $\alpha = 0.05$ unless otherwise noted.

We explored associations between gas flux rates, EEA, and porewater chemistry in year 1 (2014–2015) using Spearman's rank-order correlation (ρ) for un-transformed data as well as linear regressions to compare patterns between the four enzymes. The influence of physiochemical parameters (Cl^-, SO_4^{2-}, DIN, PO_4^-, air temperature) and productivity (GEP) on measured gas exchange rates and EEA was explored using forward stepwise multiple linear regression for the same time period.

Results

Porewater chemistry

Prior to the start of the treatments, porewater Cl^- was the same in all plots (28 ± 4 mg Cl^- L^{-1}) and increased significantly in press plots to 173 ± 40 mg Cl^- L^{-1} in April 2014, 2 weeks after treatments were initiated (Fig. 2a). Porewater Cl^- in the press plots increased to a

maximum of 1599 ± 463 mg Cl^- L^{-1} in October 2014 and remained elevated throughout the experiment. At the end of the 2-month pulse treatment in October 2014, porewater Cl^- in the pulse plots increased to 1300 ± 395 mg Cl^- L^{-1} and was not significantly different from concentrations in the press plots. By December 2014, 2 months after the end of the pulse period, Cl^- concentrations in the pulse plots fell back to control levels. These patterns continued until October 2016, when a natural seawater intrusion event raised the porewater Cl^- concentrations to at least 236 mg L^{-1} in all plots and only the pulse treatment was significantly different from the others.

Porewater SO_4^{2-} prior to the start of water additions was 1.54 ± 0.3 mg S L^{-1} and did not differ between plots (Fig. 2b). Sulfate concentrations in the press plots increased to 7.3 ± 3 mg S L^{-1} within 2 weeks of treatment initiation and were significantly higher than all other treatments for the remainder of the experiment, except in October 2014 and Oct. 2016. Porewater SO_4^{2-} was elevated in the pulse plots during the seawater pulses in Oct. 2014, Oct. 2015, and Oct. 2016. However, it was statistically significant from other treatments only during Oct. 2016.

Porewater DOC was variable (but not significantly different) between plots prior to experimental water additions (7.1–10.2 mg C L^{-1}; Fig. 2c). In the first year of treatments, DOC in both press and pulse plots showed a similar response to salinity in which DOC declined immediately following seawater application (April 2014 for press plots and October 2014 for pulse plots) but increased in later months (July and October 2014 for press and December 2014 for pulse). By March 2015, pulse plots had similar DOC concentrations to fresh and control plots (between 11.4 and 13.6 mg C L^{-1}) but press plots had significantly lower DOC concentrations (6.9 ± 3 mg C L^{-1}). For the remainder of the experiment, DOC did not show consistent patterns in either the press or the pulse plots.

Porewater DIN was between 2–7 μg N L^{-1} in all plots prior to water additions (Fig. 2d). In press plots, DIN exhibited a significant increase to 15 ± 3.8 μg N L^{-1} in July 2014 and remained elevated, but extremely variable between plots, through October 2016. DIN in pulse plots was slightly elevated during the seawater pulse in October 2014, but was never significantly different from the freshwater and control plots. Throughout the experiment, > 90% DIN was NH_4^+.

DIP was similar amongst all treatments through July of 2014 (10–30 μg P L^{-1}; Fig. 2e). In October 2014 DIP increased to 65.3 ± 15 μg P L^{-1} in the press plots and then declined in December 2014 and was not significantly different from other treatments in March and July 2015. After that it remained elevated relative to the other treatments. The seawater pulse had no significant effects on DIP. The blocking factor was significant for all porewater chemistry ($p < 0.05$) as concentrations were more diluted in the lower-elevation plots than in the higher elevation plots.

C-Acquiring enzyme activity

The activities of all four C-acquiring enzymes (BG, CB, XLY, NAG) were positively related to one another ($r^2 > 0.37$, $p < 0.001$; Fig. 8 in Supplementary Materials) so, to simplify presentation, we summed their activities (∑EEA) for each plot at each sampling date. Prior

to experimental water additions, there were no significant differences in ∑EEA between treatment groups (Fig. 3). In the winter months, ∑EEA was < 150 nmole g dry soil^{-1} h^{-1} and peaked in June and July 2014 between 335 and 559 nmole g dry soil^{-1} h^{-1}. While ∑EEA appeared to be lower in press plots than other plots after the experimental water additions began, it was highly variable, limiting our ability to detect any treatment effects. By March 2015, ∑EEA was 53% lower in the press plots than in the control and freshwater plots ($p < 0.05$). The pulse treatment showed no significant response to the 2-month saltwater addition in October, however in March 2015 after the pulse, ∑EEA was 50% higher in pulse plots than control or freshwater plots.

Gas flux

Gross ecosystem productivity remained similar in all plots until July 2014, 3 months after the press treatment began, when GEP in press plots was 30% lower than control plots ($p < 0.05$; Fig. 4a). GEP was significantly lower in press plots than in other treatments ($p < 0.05$) for all other sampling dates except October 2014 ($p < 0.10$) and March 2016 (no significant differences). Annual estimated GEP for the first year of the study (April 2014–March 2015) was 24% lower in the press plots than other treatments ($p = 0.03$; Table 2). Gross ecosystem productivity peaked in June and July of 2013, 2014, and 2016 between 9.9 and 25.7 g C m^{-2} d^{-1} and fell to 0.6–9.1 g C m^{-2} d^{-1} in December and January.

Ecosystem respiration was strongly correlated with GEP ($\rho = 0.93$, $p < 0.0001$; Table 3) and followed a similar trend as GEP (Fig. 4b). ER in press plots relative to control plots was 12% lower in June 2014 and ~ 30% lower in December 2014. Annual estimated ER for the first year of the study was 25% lower in the press plots than control plots ($p = 0.04$; Table 2). In 2015 and 2016, ER in press plots continued to decline relative to control plots. The highest rates of ER were in June and July, between 4.5 and 20.8 g C m^{-2} d^{-1} (Fig. 4b). Wintertime ER ranged from 0 to 7.3 g C m^{-2} d^{-1}.

The declines in GEP and ER in the press plots corresponded to a 27–40% decrease in NEP compared to control plots between July and December of 2014 ($p < 0.1$; Fig. 4c). Annual estimated NEP for the first year of the study was 26% lower in the press plots than control plots, but was significant only at $\alpha = 0.1$ ($p = 0.07$; Table 2). NEP was also significantly lower in press plots than control plots in June and October of 2016 ($p < 0.1$; Fig. 4c). Net ecosystem productivity was generally highest in summer months and decreased to between − 2.8 and 2.7 g C m^{-2} d^{-1} in the winter months.

Seawater additions decreased CH_4 emissions in the press plots 55% by July 2014, but this difference was not statistically significant due to high variability between replicates in all treatments (Fig. 4d). By October of 2014, CH_4 emissions were 70% lower in press plots than control plots ($p < 0.05$) and CH_4 emissions remained significantly lower in press plots than in other treatments through June 2016. Annual estimated CH_4 emissions for the first year of the study were 72% lower in the press plots than control plots (Table 2). Methane emissions were highest in July 2014 and June 2016, but were highly variable, between 1.2 and 5.7 g C m^{-2} d^{-1} and were an order of magnitude lower in the winter and spring months, < 0.6 g C m^{-2} d^{-1}.

We observed no consistent differences in gas exchange between the control, control sides, freshwater addition, and pulse treatment plots. Modeled gas fluxes were similar among plots during the pre-treatment period (Fig. 4) but did show strong gradients based on plot elevation (block), with higher gas exchange rates in lower elevation plots ($p < 0.01$).

Relationships among variables

Porewater SO_4^{2-} and Cl^- were highly correlated ($\rho = 0.96$, $p < 0.001$) and along with PO_4^- were the only variables not significantly related to temperature (Table 3). Gas exchange rates (GEP, ER, CH_4), ∑EEA and porewater DIN were all highly correlated with temperature ($\rho > 0.47$, $p < 0.01$ for all). Porewater DIN and PO_4^- were positively correlated with porewater SO_4^{2-} and Cl^- ($\rho > 0.43$, $p < 0.01$), while DOC was negatively, but not significantly, correlated with SO_4^{2-} and Cl^- concentrations. Dissolved organic C was most strongly correlated with ∑EEA and GEP ($\rho = 0.69$, $p < 0.001$ for both).

GEP was positively correlated with temperature and negatively correlated with porewater SO_4^{2-}, Cl^-, and DIN (Table 3). The best-fit model of GEP explained 83% of the variation using 3 variables: porewater Cl^- ($b = -0.0506$, $p = 0.03$), SO_4^{2-} ($b = -0.0818$, $p = 0.004$), and temperature ($b = 0.847$, $p = 0.001$; Table 4). Ecosystem respiration was significantly and positively correlated with GEP, ∑EEA and DOC (Table 3), with the best-fit model explaining 93% of the variation in ER using only GEP ($b = 0.834$, $p < 0.0001$; Table 4). Methane emissions were positively correlated with GEP, ER, porewater DOC and ∑EEA and negatively correlated with porewater SO_4^{2-} and DIN. The best-fit model using GEP ($b = 0.122$, $p = 0.006$) and temperature ($b = -0.513$, < 0.001; Table 4) explained 78% of the variation in CH_4 emissions. Finally, while ∑EEA was correlated with several potential drivers such as GEP, porewater DOC, DIN and SO_4^{2-}, and temperature (Table 3), the best-fit model explained 87% of the variation in ∑EEA using 2 variables, SO_4^{2-} ($b = -0.950$, $p < 0.001$) and GEP ($b = 23.97$, $p < 0.001$; Table 4).

Discussion

Effectiveness of treatments

Aside from the plots that were discontinued after March 2015, we successfully elevated the salinities in the press and pulse plots into the range of an oligohaline marsh (0.5–5 psu). Salinity remained significantly higher in the press plots than in the other treatments in all porewater sampling months except October 2016, when Hurricane Matthew's storm surge pushed waters of 20 psu into our study site (C. Craft, personal observation). The pulse plots also had significantly higher salinities than control and fresh plots during the pulse months (September–October) each year (Fig. 2a).

Changes in porewater chemistry

Concentrations of porewater SO_4^{2-} and Cl^- increased with salinity. While Cl^- is a conservative element (i.e. not required in large amounts by organisms), SO_4^{2-} is reduced to HS and H_2S by sulfate-reducing bacteria and abiotically combines with ferrous iron (Fe^{2+}) to form FeS and FeS_2 (Rickard and Morse 2005; Tobias and Neubauer 2009). The complexation of H_2S with Fe^{2+} causes the dissolution of Fe-PO_4 minerals, resulting in

release of PO_4^- (Paludan and Morris 1999; Lamers et al. 2001; van Diggelen et al. 2014). Sulfate-driven increases in mineralization have also been suggested to liberate P from organic matter (Williams et al. 2014).

Sodium and other seawater cations can displace NH_4^+ from soil exchange sites (Gardner et al. 1991; Rysgaard et al. 1999; Weston et al. 2010; Jun et al. 2013) and shift microbial nitrate metabolism from denitrification (NO_3^- reduced to N_2) to dissimilatory NO_3^- reduction to NH_4^+ (DNRA; Burgin and Hamilton 2007; Giblin et al. 2010). Furthermore, increased SO_4^{2-} reduction associated with salinization enhances organic matter mineralization rates because it is more energetically efficient for microbial metabolism than methanogenesis, which often dominates TFMs (Capone and Kiene 1988; Weston et al. 2006, 2011). The combination of increased N mineralization, DNRA, and ionic displacement have been observed to increase N export due to both chronic and acute saltwater intrusion (Weston et al. 2010; Giblin et al. 2010; Ardón et al. 2013). Interestingly, both press and pulse plots did not show large increase in DIN until ~ 4 months after initial saltwater addition, even though salinity was no longer elevated in pulse plots. Ionic exchange occurs within hours of seawater intrusion (Gardner et al. 1991; Weston et al. 2010), yet initial increases in DIN were small. Dissolved inorganic N was negatively correlated with GEP and positively correlated with microbial activity (∑EEA), suggesting that mineralization and low plant uptake may play a role in regulating DIN release from salinizing TFM soils.

Porewater DOC decreased immediately in both press and pulse plots following seawater addition, then increased in the 3–4 months afterwards. The immediate decrease in DOC observed in both the press and pulse plots could be due to rapid increases in C mineralization via SO_4^{2-} reduction, increased DOC flocculation (Asmala et al. 2014; Ardón et al. 2016) or stress-induced reductions in C inputs into the soil by plants. Chambers et al. (2013b) observed declines in DOC after a brackish (13 psu) pulse to an unvegetated freshwater soil core in the laboratory, and combined with our observations, this suggests that enhanced flocculation may be the most likely mechanism for reduced DOC in salinizing soils (Ardón et al. 2016). Increased DOC in the 3–4 months following initial seawater additions to the pulse plots corresponded to observed declines in GEP (Fig. 4a) and widespread mortality of the understory dominants *L. repens, P. cordata* and multiple *Polygonum* species. We suggest increased DOC was related to the mineralization of dead plant material. By March 2015, DOC was lowest in the press plots in which the majority of the vegetation was dying or dead, limiting the inputs of DOC to the plot and coinciding with reduced GEP and reduced enzyme activity. After March 2015, DOC did not show consistent trends in press or pulse plots, further confounding our interpretation of how salinization affects carbon in marsh soils.

Enzyme activity

While we saw increased SO_4^{2-} reduction as evidenced by increased HS^- in the press plots (18 mg/L versus 0.2–1.2 mg/L in the other treatments in Oct. 2014, Widney et al. in review), we did not detect increases in ER or C-acquiring enzymes due to seawater additions. Morrissey et al. (2014) showed that salinity was positively correlated with C-acquiring EEAs across estuarine salinity gradients and suggested salinity enhances enzyme-mediated

organic matter hydrolysis due to enhanced organic matter availability, enhanced energetic efficiency of metabolic pathways, and altered community structure driven by salinity and SO_4^{2-}. However, Morrissey et al.'s observational study results conflict with field and laboratory manipulations of bare soils that show decreases or no change in C-acquiring EEAs in response to salinity (Jackson and Vallaire 2009; Neubauer et al. 2013; Chambers et al. 2013a).

In the first year of our experiment, ∑EEA was negatively correlated with Cl^- and SO_4^{2-} and ∑EEA was associated with increased GEP and DOC. Enzyme activities did not decline in response to short-term salinization (early press or pulse), but instead declined in the press plots as GEP declined. However that decline was only significant for the last time point (March 2015). Enzyme activity has been linked to both C and O_2 availability in wetland soils (Kang and Freeman 1999; Shackle et al. 2000; Kang et al. 2005; Kong et al. 2009), and declines in macrophyte biomass and productivity likely reduced C and O_2 delivery to soils, decreasing labile substrate availability for microbial enzyme production. Our findings suggest that patterns in EEAs across estuarine landscapes observed by Morrissey et al. (2014) may not be consistent with disturbance-type responses observed in field experiments by Neubauer et al. (2013) and in our experiment, and that the response to salinity is mediated by changes in plant community rather than enhanced SO_4^{2-} reduction. However, our measurements of enzyme activity are likely an underestimation of the surface activity due to the deep (25 cm) depth of sampling.

Carbon flux

Press seawater additions reduced GEP. This effect was most pronounced in the middle of the growing season (June and July) and was less apparent in October when plants reach maximum biomass in coastal Georgia but physiological processes slow as leaves begin to senesce (Birch and Cooley 1982). Decreased GEP was associated with reduced *Z. miliacea* plant height and cover as well as the near complete mortality of understory species discussed above (Fig. 5). After 3 months of dosing, *Ludwigia repens* was eradicated from the press plots while aboveground biomass of *Polygonum hydropiperoides* was reduced by 75% (Li et al. in review). By the end of the first season (2014), aboveground biomass of *Zizaniopsis miliacea* was significantly lower in the press plots compared to the controls (Li et al. in review).

The physiological tolerance of many freshwater species to salinity is low (Hart et al. 1990; Williams 1999; Nielsen et al. 2003; Munns and Tester 2008), and many studies report similar decreases in freshwater plant productivity, biomass, GEP, and leaf-level photosynthesis in response to increased salinity (Baldwin and Mendelssohn 1998; Spalding and Hester 2007; Munns and Tester 2008; Sutter et al. 2013; Hackney and Avery 2015). The herbaceous species in the plots appeared to be much more sensitive to salinity than *Z. miliacea*, which has been shown to tolerate low levels of salinity (Guo and Pennings 2012; Neubauer 2013) although it is less productive in the Altamaha estuary when freshwater flows are low (Ket et al. 2011). In a more gradual seawater intrusion event, brackish vegetation might have begun to establish as freshwater vegetation declined, mitigating the effect on GEP. The plot size and distance from brackish vegetation limited the extent to

which this was possible in our study, so our measurements may be an overestimate of the effect of seawater intrusion on GEP. Further, due to logistical considerations, our gas exchange measurements were limited to 3–5 times per year. For that reason, we have calculated annual fluxes for the most heavily sampled time period (2014–2015) only, when measurements were made during all four seasons.

The 72% reduction in CH_4 from 132–41 g C m^{-2} $year^{-1}$ in the first year of treatments was not large enough to shift the press plots from a source of greenhouse gases into a sink. Even so, based on global warming potentials of Neubauer and Megonigal (2015), chronic salinization reduced net radiative forcing of the site from 5491 g CO_2 equivalent m^{-2} $year^{-1}$–1579 g CO_2 equivalent m^{-2} $year^{-1}$ within the first year of treatments. Despite some seasonal variability, observed reductions in GEP, ER, NEP, and CH_4 in the press plots continued through 2015 and 2016, suggesting that chronic seawater intrusion will lead to reduced C fixation in tidal freshwater marshes.

Perhaps the greatest effect of saltwater intrusion is the decline and loss of emergent vegetation (Li et al. in review). Decreased productivity not only reduces the C storage potential of these systems, but may reduce their resilience to sea level rise by inducing soil subsidence (Neubauer 2013). TFMs rely on organic matter deposition to build soil volume against rising sea levels (Neubauer 2008) and aboveground biomass is important for trapping sediment to support vertical accretion (Morris et al. 2002).

Conclusions

After 2.5 years of simulated seawater intrusion in a TFM, we found that chronic increases in salinity caused an increase in porewater Cl^-, SO_4^{2-}, DIN, and DIP, but substrate SO_4 availability did not appear to enhance microbial mineralization or enzyme activity. Instead, we observed that decreased enzyme activity (50%) and ER (25%) were more closely linked to a decline in GEP (− 24%) in press plots. Despite high productivity in the control plots, high CH_4 emissions made the site a net source of greenhouse gases. Press seawater additions decreased CH_4 emissions by 72% within the first year of treatments, likely through a combination of direct suppression by SO_4^{2-} reduction and indirect suppression mediated by declining plant productivity. Mimicking natural late-fall seawater intrusion in the pulse treatment revealed that, while salinity pulses had similar effects on porewater chemistry as press seawater additions, they had no discernable effect on gas exchange. Both press and pulse salinity released inorganic N and P into the porewater, where they can potentially be exported downstream.

Supplementary Material

Refer to Web version on PubMed Central for supplementary material.

Acknowledgements

We thank the students and technicians who participated in the SALTEx project, especially Dontrece Smith, M. Maurer, C. Peacock, and the many IU Wetlands Laboratory students and GCE LTER Schoolyard participants who helped build the porewater wells and measure porewater and gas fluxes. A special thanks to Sarah Widney and two anonymous reviewers who made substantive improvements to the manuscript. This research was supported by

funding from the National Science Foundation to CBC through the NSF LTER program (Georgia Coastal Ecosystems LTER, OCE-9982133, OCE-0620959 and OCE-1237140) and to ERH through the NSF GRFP (2011117001) and NSF DEB DDIG program (DEB-1401070) and support from the U.S. EPA ORD to JSB. This is contribution 1065 of the University of Georgia Marine Institute. The views expressed in this paper are those of the authors and do not necessarily reflect the views or policies of the USEPA.

References

Allison SD, Vitousek PM (2005) Responses of extracellular enzymes to simple and complex nutrient inputs. Soil Biol Biochem 37:937–944

Ardón M, Morse JL, Colman BP, Bernhardt ES (2013) Drought-induced saltwater incursion leads to increased wetland nitrogen export. Glob Change Biol 19:2976–2985

Ardón M, Helton AM, Bernhardt ES (2016) Drought and saltwater incursion synergistically reduce dissolved organic carbon export from coastal freshwater wetlands. Biogeochemistry 127(2–3):411–426

Asmala E, Bowers DG, Autio R, Kaartokallio H, Thomas DN (2014) Qualitative changes of riverine dissolved organic matter at low salinities due to flocculation. Biogeosciences 119:1919–1933

Baldwin AH, Mendelssohn IA (1998) Effects of salinity and water level on coastal marshes: an experimental test of disturbance as a catalyst for vegetation change. Aquat Bot 61:255–268

Barendregt A, Whigham D, Baldwin A (2009) An introduction to the ecosystem In: Barendregt A, Whigham D, Baldwin A () Tidal freshwater wetlands. Backhuys-Weikersheim, Leiden

Bartlett KB, Bartlett DS, Harriss RC, Sebacher DI (1987) Methane emissions along a salt marsh salinity gradient. Biogeochemistry 4:183–202

Bell CW, Fricks BE, Rocca JD, Steinweg JM, McMahon SK, Wallenstein MD (2013) High-throughput fluorometric measurement of potential soil extracellular enzyme activities. J Vis Exp 81:e50961

Birch JB, Cooley JL (1982) Production and standing crop patterns of giant cutgrass (Zizaniopsis miliacea) in a freshwater tidal marsh. Oecologia 52(2):230–235 [PubMed: 28310513]

Burgin AJ, Hamilton SK (2007) Have we overemphasized denitrification in aquatic ecosystems? A review of nitrate removal pathways. Front Ecol Environ 5:89–96

Capone GD, Kiene RP (1988) Comparison of microbial dynamics in marine and freshwater sediments: contrasts in anaerobic carbon catabolism. Limnol Oceanogr 33(4, part 2):725–749

Chambers LG, Reddy KR, Osborne TZ (2011) Short-term response of carbon cycling to salinity pulses in a freshwater wetland. Soil Sci Soc Am J 75:2000–2007

Chambers LG, Davis SE, Troxler T, Boyer JN, Downey-Wall A, Scinto LJ, Scinto ADLJ (2013a) Biogeochemical effects of simulated sea level rise on carbon loss in an Everglades mangrove peat soil. Hydrobiologia 726:195–211

Chambers LG, Osborne TZ, Reddy KR (2013b) Effect of salinity-altering pulsing events on soil organic carbon loss along an intertidal wetland gradient: a laboratory experiment. Biogeochemistry 115:363–383

Church JA, Clark PU, Cazenave A, Gregory JM, Jevrejeva S, Levermann A, Merrifield MA, Milne GA, Nerem RS, Nunn PD, Payne AJ, Pfeffer WT, Stammer D, Unnikrishnan AS (2013) Sea Level Change In: Stocker TD, Qin D, Plattner GK, Tignor M, Allen SK, Boschung J, Nauels A, Xia Y, Bex V, Midgley PM () Climate Change 2013: The Physical Science Basis. Contribution of Working Group I to the Fifth Assessment Report of the Intergovernmental Panel on Climate Change 1137–1216

Craft C (2007) Freshwater input structures soil properties, vertical accretion, and nutrient accumulation of Georgia and U.S tidal marshes. Limnol Oceanogr 52:1220–1230

Edmonds JW, Weston NB, Joye SB, Mou X, Moran MA (2009) Microbial community response to seawater amendment in low-salinity tidal sediments. Microb Ecol 58:558–568 [PubMed: 19629578]

Flynn KM, McKee KL, Mendelssohn IA (1995) Recovery of freshwater marsh vegetation after a saltwater intrusion event. Oecologia 103:63–72 [PubMed: 28306946]

Freeman C, Nevison G, Hughes S, Reynolds B, Hudson J (1998) Enzymatic involvement in the biogeochemical responses of a Welsh peatland to a rainfall enhancement manipulation. Biol Fertil Soils 27:173–178

Gardner WS, Seitzinger SP, Malczyk JM (1991) The effects of sea salts on the forms of nitrogen released from estuarine and freshwater sediments: does ion pairing affect ammonium flux? Estuaries 14:157–166

Giblin AE, Weston NB, Banta GT, Tucker J, Hopkinson CS (2010) The effects of salinity on nitrogen losses from an oligohaline estuarine sediment. Estuar Coasts 33:1054–1068

Guo H, Pennings SC (2012) Mechanisms mediating plant distributions across estuarine landscapes in a low-latitude tidal estuary. Ecology 93:90–100 [PubMed: 22486090]

Hackney CT, Avery GB (2015) Tidal wetland community response to varying levels of flooding by saline water. Wetlands 35:227–236

Hart BT, Bailey P, Edwards R, Hortle K, James K, Mcmahon A, Meredith C (1990) Effects of salinity on river, stream and wetland ecosystems in Victoria, Austraila. J Water Res 24:1103–1117

Herbert E, Boon P, Burgin AJ, Neubauer SC, Franklin RB, Ardon M, Hopfensperger KN, Lamers L, Gell P (2015) A global perspective on wetland salinization: ecological consequences of a growing threat to freshwater wetlands. Ecosphere 6(10):206

Hopkinson CS (1992) A comparison of ecosystem dynamics in freshwater wetlands. Estuaries 15:549

Horton BP, Rahmstorf S, Engelhart SE, Kemp AC (2014) Expert assessment of sea-level rise by AD 2100 and AD 2300. Quat Sci Rev 84:1–6

Jackson CR, Vallaire SC (2009) Effects of salinity and nutrients on microbial assemblages in Louisiana wetland sediments. Wetlands 29:277–287

Johns C, Ramsey M, Bell D, Vaughton G (2014) Does increased salinity reduce functional depth tolerance of four non-halophytic wetland macrophyte species? Aquat Bot 116:13–18

Jun M, Altor AE, Craft CB (2013) Effects of increased salinity and inundation on inorganic nitrogen exchange and phosphorus sorption by tidal freshwater floodplain forest soils, Georgia (USA). Estuar Coasts 36:508–518

Kang H, Freeman C (1999) Phosphatase and arylsulphatase activities in wetland soils: annual variation and controlling factors. Soil Biol Biochem 31:449–454

Kang H, Kim SY, Fenner N, Freeman C (2005) Shifts of soil enzyme activities in wetlands exposed to elevated CO_2. Sci Total Environ 337:207–212 [PubMed: 15626391]

Ket WA, Schubauer-Berigan JP, Craft CB (2011) Effects of five years of nitrogen and phosphorus additions on a Zizaniopsis miliacea tidal freshwater marsh. Aquat Bot 95:17–23

Kong L, Wang YB, Zhao LN, Chen ZH (2009) Enzyme and root activities in surface-flow constructed wetlands. Chemosphere 76:601–608 [PubMed: 19497608]

Lamers LPM, Els Ten Dolle G, Van Den Berg STG, Van Delft SPJ, Roelofs JGM (2001) Differential responses of freshwater wetland soils to sulphate pollution. Biogeochemistry 55:87–102

Lamers LPM, Govers LL, Janssen ICJM, Geurts JJM, Van der Welle MEW, Van Katwijk MM, Van der Heide T, Roelofs JGM, Smolders AJP (2013) Sulfide as a soil phytotoxin-a review. Front Plant Sci 4:268 [PubMed: 23885259]

Lamers LPM, Falla S, Samborska EM, Van Dulken IAR, Hengstum V, Roelofs JGM (2014) Factors controlling the extent of eutrophication and toxicity in sulfate-polluted freshwater wetlands. Limnol Oceanogr 47:585–593

Lovley DR, Klug MJ (1986) Model for the distribution of sulfate reduction and methanogenesis in freshwater sediments. Geochim Cosmochim Acta 50:11–18

Madrid EN, Armitage AR, Quigg A (2012) The response of photosystem II to soil salinity and nutrients in wetland plant species of the northwestern Gulf of Mexico. J Coast Res 284:1197–1207

Marton JM, Herbert ER, Craft CB (2012) Effects of salinity on denitrification and greenhouse gas production from laboratory-incubated tidal forest soils. Wetlands 32:347–357

Montagna PA, Alber M, Doering P, Connor MS (2002) Freshwater inflow: science, policy, management. Estuaries 25:1243–1245

Morris JT, Sundareshwar PV, Nietch CT, Kjerve B, Cahoon DR (2002) Responses of coastal wetlands to rising sea level. Ecology 83:2869–2877

Morrissey EM, Berrier DJ, Neubauer SC, Franklin RB (2013) Using microbial communities and extracellular enzymes to link soil organic matter characteristics to greenhouse gas production in a tidal freshwater wetland. Biogeochemistry 117:473–490

Morrissey EM, Gillespie JL, Morina JC, Franklin RB (2014) Salinity affects microbial activity and soil organic matter content in tidal wetlands. Glob Change Biol 20:1351–1362

Munns R, Tester M (2008) Mechanisms of salinity tolerance. Annu Rev Plant Biol 59:651–681 [PubMed: 18444910]

Nelson TM, Streten C, Gibb KS, Chariton AA (2015) Saltwater intrusion history shapes the response of bacterial communities upon rehydration. Sci Total Environ 502:143–148 [PubMed: 25247483]

Neubauer SC (2008) Contributions of mineral and organic components to tidal freshwater marsh accretion. Estuarine 78:78–88

Neubauer SC (2013) Ecosystem responses of a tidal freshwater marsh experiencing saltwater intrusion and altered hydrology. Estuar Coasts 36:491–507

Neubauer SC, Craft CB (2009) Global change and tidal freshwater wetlands: scenarios and impacts In: Barendregt A, Whigham D, Baldwin A () Tidal freshwater wetlands. Backhuys-Weikersheim, Leiden, 253–266

Neubauer SC, Megonigal JP (2015) Moving beyond global warming potentials to quantify the climatic role of ecosystems. Ecosystems 18(6):1000–1013

Neubauer SC, Miller DW, Anderson IC (2000) Carbon cycling in a tidal freshwater marsh ecosystem: a carbon gas flux study. Mar Freshw Res 199:13–30

Neubauer SC, Givler K, Valentine S, Megonigal JP (2005) Seasonal patterns and plant-mediated controls of subsurface wetland biogeochemistry. Ecology 86:3334–3344

Neubauer SC, Franklin RB, Berrier DJ (2013) Saltwater intrusion into tidal freshwater marshes alters the biogeochemical processing of organic carbon. Biogeosciences 10:10685–10720

Nielsen DL, Brock MA, Rees GN, Baldwin DS (2003) Effects of increasing salinity on freshwater ecosystems in Australia. Aust J Bot 51:655

Nijssen B, O'Donnell GM, Hamlet AF, Lettenmaier DP (2001) Hydrologic sensitivity of global rivers to climate change. Clim Change 50:143–175

Noe GB, Krauss KW, Lockaby BG, Conner WH, Hupp CR (2013) The effect of increasing salinity and forest mortality on soil nitrogen and phosphorus mineralization in tidal freshwater forested wetlands. Biogeochemistry 114:225–244

Odum W (1988) Comparative ecology of tidal freshwater and salt marshes. Annu Rev Ecol Syst 19:147–176

Paludan C, Morris JT (1999) Distribution and speciation of phosphorus along a salinity gradient in intertidal marsh sediments. Biogeochemistry 45:197–221

Parris A, Bromirski P, Burkett V, Cayan D, Culver M, Hall J, Horton R, Knuuti K, Moss R, Obeysekera J, Sallenger A, Weiss J (2012) Global Sea Level Rise Scenarios for the United States National Climate Assessment NOAA Technical Report OAR CPO-1. Climate Program Office, Silver Springs, MD, USA

Poffenbarger HJ, Needelman BA, Megonigal JP (2011) Salinity influence on methane emissions from tidal marshes. Wetlands 31:831–842

Prat N, Ibanez C (1995) Effects of water transfers projected in the Spanish National Hydrological Plan on the ecology of the lower river Ebro (N.E. Spain) and its delta. Water Sci Technol 31:79–86

Rickard D, Morse JW (2005) Acid volatile sulfide (AVS). Mar Chem 97:141–197

Rysgaard S, Thastum P, Dalsgaard T, Christensen PB, Sloth NP, Rysgaard S (1999) Effects of salinity on NH_4^+ adsorption capacity, nitrification, and denitrification in Danish estuarine sediments. Estuaries 22:21

Schimel JP, Weintraub MN (2003) The implications of exoenzyme activity on microbial carbon and nitrogen limitation in soil: a theoretical model. Soil Biol Biochem 35:549–563

Segarra KEA, Comerford C, Slaughter J, Joye SB (2013) Impact of electron acceptor availability on the anaerobic oxidation of methane in coastal freshwater and brackish wetland sediments. Geochim Cosmochim Acta 115:15–30

Shackle VJ, Freeman C, Reynolds B (2000) Carbon supply and the regulation of enzyme activity in constructed wetlands. Soil Biol Biochem 32:1935–1940

Sharpe PJ, Baldwin AH (2012) Tidal marsh plant community response to sea-level rise: a mesocosm study. Aquat Bot 101:34–40

Sinsabaugh RL, Findlay S (1995) Microbial production, enzyme activity, and carbon turnover in surface sediments of the Hudson River estuary. Microb Ecol 30:127–141 [PubMed: 24185480]

Sinsabaugh RL, Moorhead DL (1994) Resource allocation to extracellular enzyme production: a model for nitrogen and phosphorus control of litter decomposition. Soil Biol Biochem 26:1305–1311

Soil Survey Staff, Natural Resources Conservation Service, United States Department of Agriculture. Web Soil Survey. https://websoilsurvey.sc.egov.usda.gov/. Accessed 4 7 2015

Spalding E, Hester M (2007) Interactive effects of hydrology and salinity on oligohaline plant species productivity: implications of relative sea-level rise. Estuar Coasts 30:214–225

Sutter LA, Perry JE, Chambers RM (2013) Tidal freshwater marsh plant responses to low level salinity increases. Wetlands 34:167–175

Sutton-Grier AE, Megonigal JP (2011) Plant species traits regulate methane production in freshwater wetland soils. Soil Biol Biochem 43:413–420

Tobias C, Neubauer SC (2009) Saltmarsh biogeochemistry: an overview In: Perillo GME, Wolanski E, Cahoon DR, Brinson MM () Coastal wetlands: an integrated ecosystem approach. Elsevier, Amsterdam, 445–492

Van Der Nat FJWA, Middelburg JJ (1998) Effects of two common macrophytes on methane dynamics in freshwater sediments. Biogeochemistry 43:79–104

Van Diggelen JMH, Lamers LPM, van Dijk G, Schaafsma MJ, Roelofs JGM, Smolders AJP (2014) New insights into phosphorus mobilisation from sulphur-rich sediments: time-dependent effects of salinisation. PLoS ONE 9:e111106 [PubMed: 25369128]

Weston NB, Dixon RE, Joye SB (2006) Ramifications of increased salinity in tidal freshwater sediments: geochemistry and microbial pathways of organic matter mineralization. J Geophys Res 111:G01009

Weston NB, Giblin AE, Banta GT, Hopkinson CS, Tucker J (2010) The effects of varying salinity on ammonium exchange in estuarine sediments of the Parker River, Massachusetts. Estuar Coasts 33:985–1003

Weston NB, Vile MA, Neubauer SC, Velinsky DJ (2011) Accelerated microbial organic matter mineralization following salt-water intrusion into tidal freshwater marsh soils. Biogeochemistry 102:135–151

Whiting GJ, Bartlett DS, Fan SM, Bakwin PS, Wolfsy SC (1992) Biosphere atmosphere CO2 exchange in tundra ecosystems – community characteristics and relationships with multispectral surface reflectance. J Geophys Res 97(D15):16671–16680

Williams WD (1999) Salinisation: a major threat to water resources in the arid and semi-arid regions of the world. Lakes Reserv 4:85–91

Williams AA, Lauer NT, Hackney CT (2014) Soil phosphorus dynamics and saltwater intrusion in a florida estuary. Wetlands 34:535–544

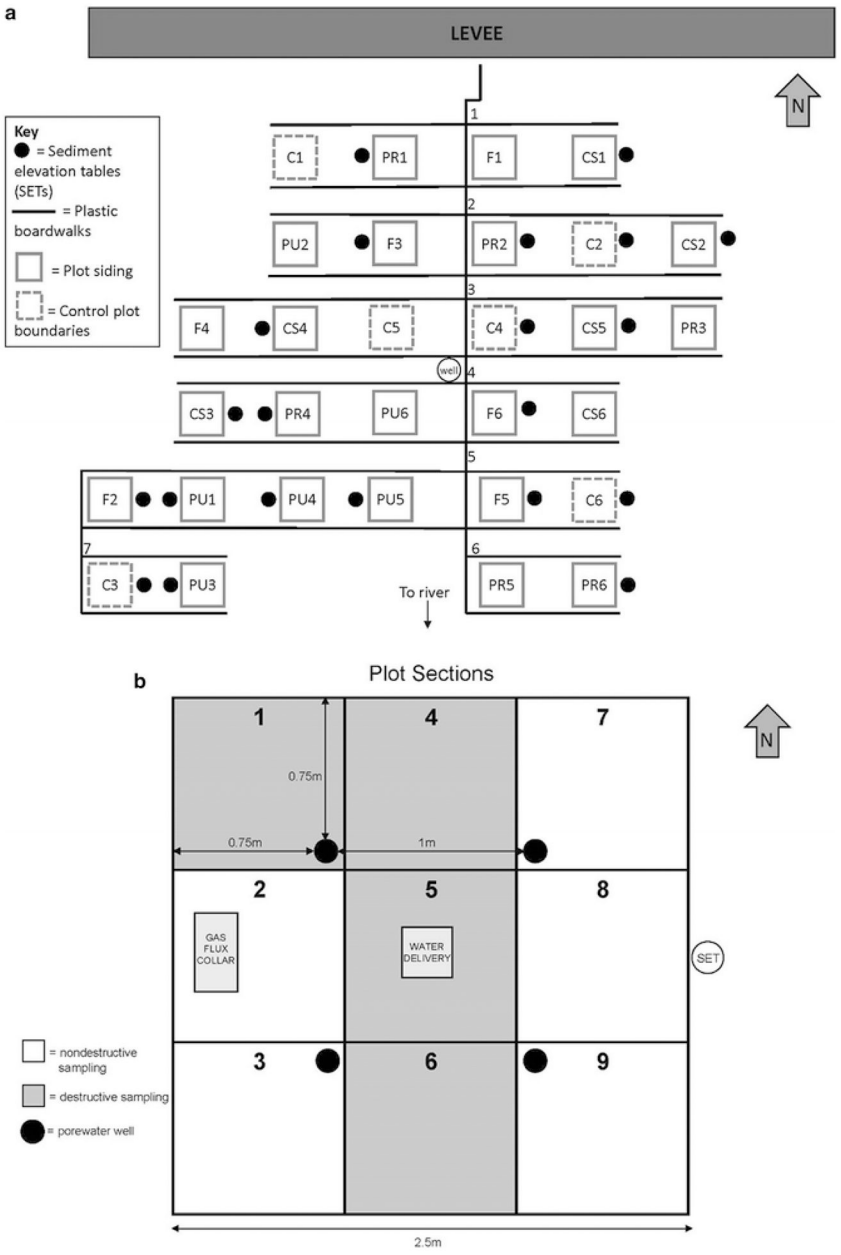

Fig. 1.

a Plot layout map for the SALTEx site. Plot names (treatment abbreviation + replicate) are indicated within the boundaries of each plot. **b** Sampling locations within the individual plots. Porewater wells are indicated with black circles, gas flux measurements were made in Sect. 2, and soil samples were collected from Sect. 6. The gas flux collar is made of ~ one inch thick aluminum siding and was moved between plots (i.e., not permanently installed) during the study period

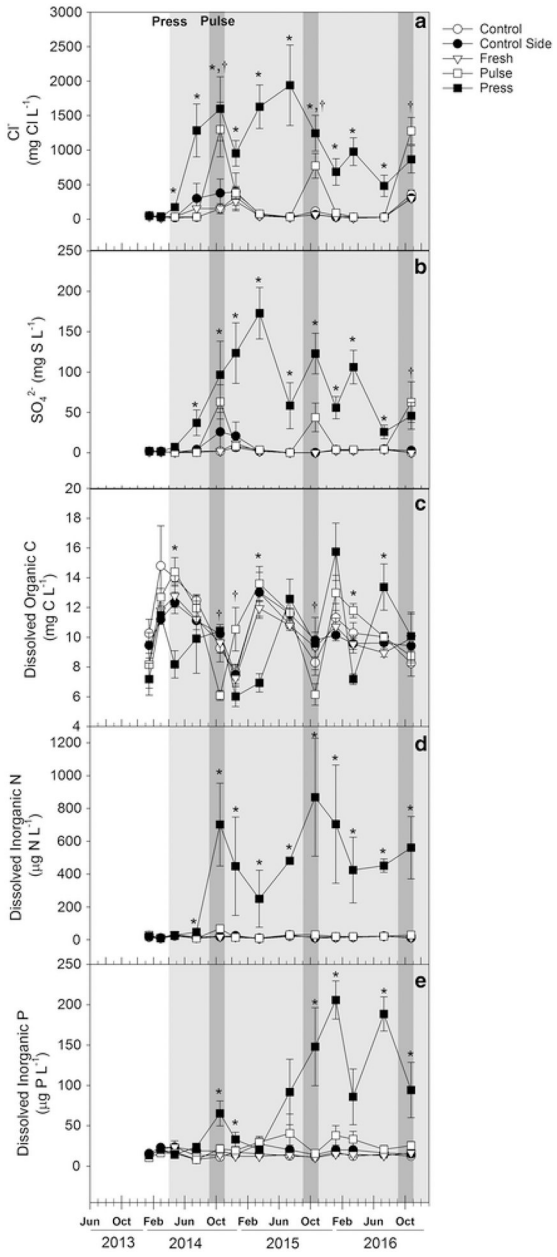

Fig. 2.

Mean porewater concentrations (± SE) of **a** Cl^-, **b** SO_4^{2-}, **c** DOC (mg L^{-1}), **d** DIN and **e** PO_4^- (µg L^{-1}) of all treatments from seasonal porewater samples. The white portion of the graph represents pre-treatment salinity, the light grey shading the press seawater addition, and the dark grey shading the simultaneous pulse and press seawater addition. Control (open circle), control sides (solid circle) and fresh (open triangle) values are not significantly different from one another ($p > 0.05$). Press (solid square) values marked with a * and pulse (open square) values marked with a † are significantly different from other treatments ($p < 0.05$; Ryan-Einot-Gabriel-Welsch Multiple Range Test)

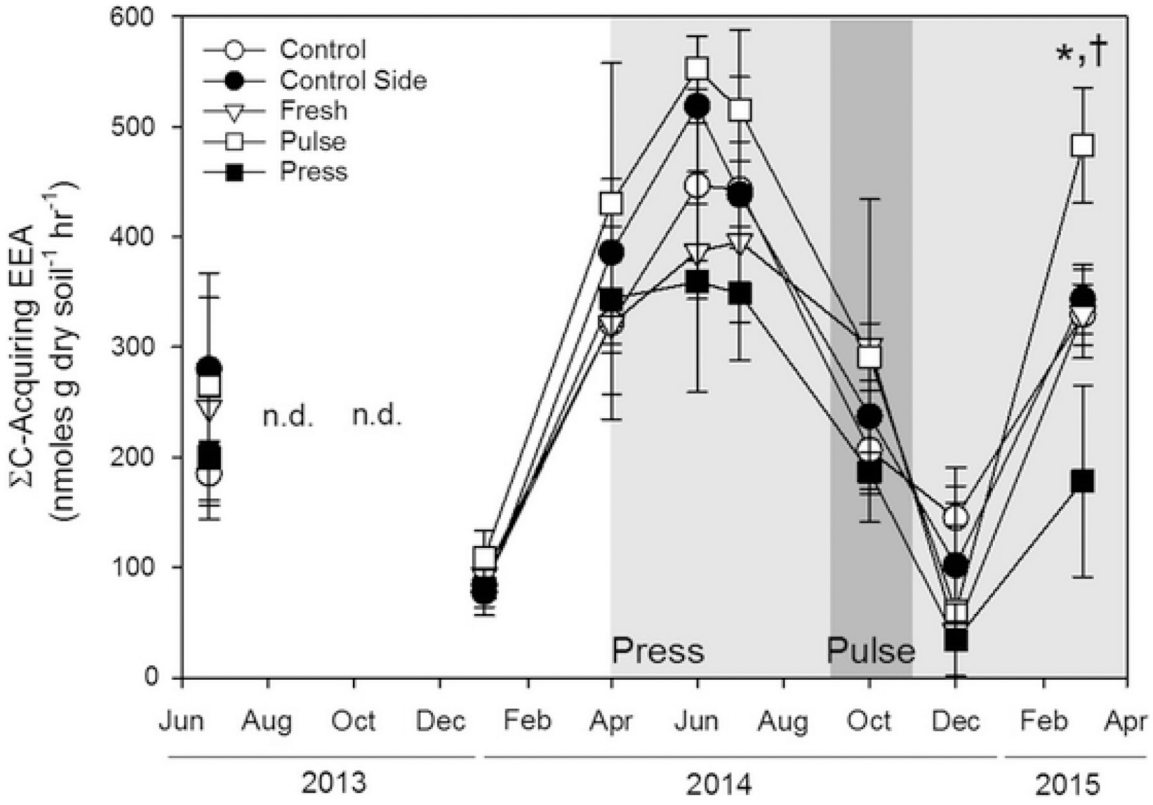

Fig. 3.

Mean C-acquiring enzyme activity (± SE) in nmoles g dry soil^{-1} h^{-1} measured seasonally in all treatments (n = 6). The white portion of the graph represents pre-treatment salinity, the light grey shading the press seawater addition, and the dark grey shading the simultaneous pulse and press seawater addition. Control (open circle), control sides (solid circle) and fresh (open triangle) values are not significantly different from one another ($p > 0.05$). Press (solid square) values marked with a * and pulse (open square) values marked with a † are significantly different from other treatments ($p < 0.05$; Ryan-Einot-Gabriel-Welsch Multiple Range Test)

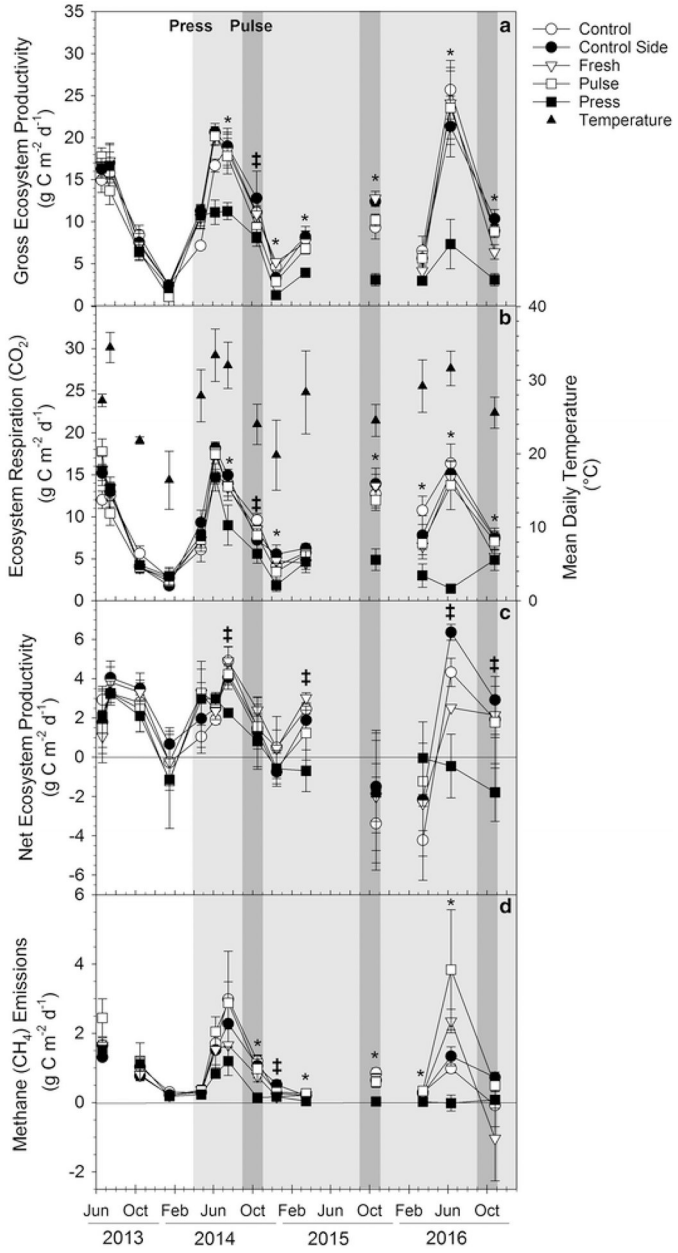

Fig. 4.

Mean modeled daily rates of **a** GEP, **b** ER, **c** NEP and **d** CH_4 emissions (± SE) in g Cm^{-2} d^{-1} calculated from field gas flux rates measured seasonally in all treatments. Solid triangles in (**b**) are mean daily air temperature (± SE). The white portion of the graph represents pre-treatment salinity, the light grey shading the press seawater addition, and the dark grey shading the simultaneous pulse and press seawater addition. Control (open circle), control sides (solid circle), fresh (open triangle) and pulse (open square) values are never significantly different from one another ($p > 0.05$). Press (solid square) values marked with a * are significantly different from other treatments at $\alpha = 0.05$ and those with a ‡ at $\alpha = 0.1$ (Ryan-Einot-Gabriel-Welsch Multiple Range Test)

Fig. 5.
Photographs of press (left) and control (right) treatment plots in July 2015 after > 1 year of experimental water additions Photo credit: Chris Craft

Table 1

Chemical composition of seawater and fresh river water mixed to make press and pulse treatment water

Water type	Salinity (psu)	NH_4 (µg-N/L)	NO_3^{-2} (µg-N/L)	PO_4 (µg-N/L)	Total N (µg-N/L)	Total P (µg-N/L)	SO_4^{2-} (mg-N/L)	DOC (mg-N/L)
Sea water	21.88 ± 1.93 (5)	14.95 ± 5.03 (5)	17.22 ± 1.62 (5)	55.94 ± 7.50 (5)	673.4 ± 98.3 (5)	71.86 ± 8.84 (5)	1914 ± 12 (2)	6.12 ± 0.56 (5)
River water	0.09 ± 0.03 (5)	56.78 ± 19.76 (6)	199.3 ± 39.06 (6)	46.43 ± 8.28 (6)	1265 ± 243 (6)	142.6 ± 52.1 (6)	36 ± 6.9 (2)	13.14 ± 2.70 (6)
Treatment water	16.24 ± 0.08 (5)	29.93 ± 2.60 (6)	98.46 ± 19.52 (6)	52.62 ± 5.53 (6)	741.0 ± 54.4 (6)	60.46 ± 5.07 (6)	1546 ± 116 (2)	8.27 ± 1.18 (6)

Mean ± SE (number of samples analyzed)

Table 2

Estimated annual C flux rates in g C m^{-2} $year^{-1}$ from plots for the first year of the study (April 2014–March 2015)

Treatment	GEP	ER	NEP	CH_4
	(g C m^{-2} $year^{-1}$)	(g C m^{-2} $year^{-1}$)	(g C m^{-2} $year^{-1}$)	(g C m^{-2} $year^{-1}$)
C	2169 ± 283[a]	1765 ± 154[a]	368 ± 61	114 ± 23[a]
CS	2434 ± 185[a]	1971 ± 220[a]	393 ± 60	100 ± 16[a]
F	2353 ± 226[a]	1806 ± 185[a]	387 ± 60	89 ± 12[b]
PU	2164 ± 345[a,b]	1745 ± 221[a,b]	360 ± 62	113 ± 9[a]
PR	1656 ± 322[b]	1356 ± 210[b]	273 ± 71	43 ± 17[c]

Treatment means (± SE) within the same column followed by the same letter are not significantly different ($p > 0.05$; Ryan-Einot-Gabriel-Welsch Multiple Range Test). SEs for GEP, ER and NEP were calculated by modeling flux rates for the six individual plots as described in the *Gas flux modeling* section with the error representing the variation between plots

Table 3

Spearman's rho (ρ) correlation coefficient for relationships between gas flux, temperature, EEA, and porewater variables

	ER	**CH_4**	**∑EEA**	**Temp**	**SO_4^{2-}**	**Cl^-**	**DOC**	**DIN**	**PO_4^-**
GEP	0.96***	0.86***	0.75***	0.77***	− 0.49*	− 0.38*	0.69***	− 0.33*	− 0.039
ER		0.89***	0.97***	0.74***	− 0.27	− 0.169	0.49**	− 0.25	− 0.06
CH_4			0.62***	0.55***	− 0.34*	− 0.21	0.31	0.12	− 0.28
∑EEA				0.77***	− 0.39*	− 0.31	0.69***	− 0.4*	012
Temp					− 0.15	− 0.06	0.58***	− 0.47**	0.12
SO_4^{2-}						0.96***	− 0.19	0.56**	0.47**
Cl^-							− 0.08	0.5**	0.43**
DOC									− 0.039
DIN									0.43**

Superscripts indicate significance:

* $p < 0.05$,

** $p < 0.01$,

*** $p < 0.001$

Table 4

Intercept, regression coefficients and r^2 for best-fit models of seasonal gross ecosystem productivity (GEP), ecosystem respiration (ER), methane emissions (CH_4) and C-acquiring enzyme activity (ΣEEA) based on forward step-wise linear regression

	Intercept	Cl^-	SO_4^{2-}	Temperature	GEP	r^2
GEP	− 12.510	− 0.00506 *	− 0.0818 **	0.847 ***	–	0.81
ER	0.153	–	–	–	0.834	0.93
CH_4	0.786	–	–	− 1.1513 ***	0.122 **	0.78
ΣEEA	− 31.592	–	− 0.95 ***	–	23.79 ***	0.87

Superscripts indicate significance of regression coefficient:

* $p < 0.05$,

** $p < 0.01$,

*** $p < 0.001$